Electron Resist Behavior of Pd Hexadecanethiolate Examined Using X-ray Photoelectron Spectroscopy with Nanometric Lateral Resolution

T. Bhuvana,[†] Luca Gregoratti,[‡] Stefan Heun,[§] Matteo Dalmiglio,[‡] and G. U. Kulkarni*,[†]

Chemistry and Physics of Materials Unit and DST Unit on Nanoscience, Jawaharlal Nehru Centre for Advanced Scientific Research, Jakkur P O, Bangalore 560 064, India, Sincrotrone Trieste ScPA, Area Science Park, SS14-Km163.5, 34012 Basovizza-Trieste, Italy, and NEST CNR-INFM and Scuola Normale Superiore, Piazza San Silvestro 12, 56127 Pisa, Italy

Received October 16, 2008. Revised Manuscript Received November 16, 2008

Electron resist behavior of Pd hexadecanethiolate is studied by varying the e-dosage from 2−280 $\mu C \cdot cm^{-2}$. The e-beam exposed resist is characterized using energy dispersive spectroscopy, infrared spectroscopy, and X-ray photoelectron spectroscopy with nanometric lateral resolution. Electron beam exposure causes defects in the alkyl chain of the thiolate, giving the required solubility contrast during the developing step, thus qualifying the precursor as an e-beam resist. On exposure to the e-beam, the reduction of Pd^{2+} to Pd^0 is observed, and the reduction increases with increasing e-dosage. The resist is highly sensitive, with the estimated sensitivity being 32 $\mu C \cdot cm^{-2}$. Thermolysis at 250 °C leads to the formation of Pd nanoparticles, demonstrating the essential feature of a direct write resist for conducting patterns.

Introduction

Site-specific fabrication of high definition metal and semiconductor nanostructures using a minimal number of process steps is still a challenge in nanolithography and fabrication.[1−7] This has led to the pursuit for nanomaterial precursors that act as resists in direct-write lithographic methods. Among various direct write methods, e-beam based techniques have become popular for high-resolution patterning.[6] Beam induced deposition techniques such as electron beam induced deposition (EBID) and focused ion beam induced deposition (FIBID) using high vapor pressure metal-organic precursors are being employed extensively.[6,7] Commonly used precursors are $W(CO)_6$,[8] $Au(acac)_2$,[9] $(MeCp)PtMe_3$,[10−12] and so forth. Developing appropriate precursors for different metals is not always easy. The precursor should easily vaporize to fill the e-beam chamber at typically 10^{-3} Torr and should crack readily under e-beam to leave the reduced metal on the substrate. The deposited metal usually contains leftover carbon as an impurity that may be up to 70% of deposited material![9−12] Although expected to be metallic, the written patterns often bear resistivity values that are few orders of magnitude higher than that of the bulk.[9−12]

There is increasing interest in the literature to come up with metal precursors that could act as direct write resists in electron beam lithography (EBL). In a solid resist based direct write method, a nanomaterial precursor is coated as a thin film on a substrate which upon exposure to e-beam undergoes chemical transformation that would change its solubility properties, qualifying it as a resist. For a metal precursor to act as a good resist, it should be amenable to coat as a smooth thin film preferably by spin-coating from the solution, a prerequisite condition which immediately rules out all insoluble or even sparingly soluble precursors. Those which form colloidal suspensions may not also serve as well, since the particle size itself brings a constraint on the achievable resolution. In addition, to serve as a direct write resist, the precursor should desirably exhibit high sensitivity to e-beam. Importantly, following a simple post treatment, it should transform into the desired nanomaterial. There have been many reports on direct write resists for metals and metal oxides. For example, Donthu et al.[13] have developed sol−gel precursors for patterning inorganic ceramic oxides such as ZnO and PZT. Subramanian et al.[14] employed zirconium *n*-butoxide mixed with benzoyl acetone in ethanol as a resist to write ZrO_2 patterns. The sensitivity of the resist was found to improve following baking the resist at 85 °C, from ∼40 to ∼9 $mC \cdot cm^{-2}$. Similarly, metal-organic precursors have been developed to obtain ZnO[15] and TiO_2[16] patterns. Chuang et al.[17] and Wu et al.[18] have developed a water-soluble resist precursor for generating $La_{0.7}Sr_{0.3}MnO_3$ nanopatterns. Colloidal preparations

* To whom correspondence should be addressed. E-mail: kulkarni@jncasr.ac.in.

† Jawaharlal Nehru Centre for Advanced Scientific Research.

‡ Sincrotrone Trieste ScPA.

§ NEST CNR-INFM and Scuola Normale Superiore.

(1) Xia, Y.; Whitesides, G. M. *Annu. Rev. Mater. Sci.* **1998**, *28*, 153.

(2) Michel, B.; Bernard, A.; Bietsch, A.; Delamarche, E.; Geissler, M.; Juncker, D.; Kind, H.; Renault, J. P.; Rothuizen, H.; Schmid, H.; Schmidt-Winkel, P.; Stutz, R.; Wolf, H. *IBM J. Res. Dev.* **2001**, *45*, 697.

(3) Ginger, D. S.; Zhang, H.; Mirkin, C. A. *Angew. Chem., Int. Ed.* **2004**, *43*, 30.

(4) Gerlach, R. L.; Utlaut, M. *J. Vac. Sci. Technol., B* **2001**, *4510*, 96.

(5) Geissler, M.; Xia, Y. *Adv. Mater.* **2004**, *16*, 1249.

(6) Tseng, A. A.; Chen, K.; Chen, C. D.; Ma, K. J. *IEEE Trans. Electron. Packag. Manuf.* **2003**, *26*, 141.

(7) Tseng, A. A. *Small* **2005**, *1*, 924.

(8) Hoyle, P. C.; Cleaver, J. R. A.; Ahmed, H. *J. Vac. Sci. Technol., B* **1996**, *14*, 662.

(9) Botman, A.; Mulders, J. J. L.; Weemaes, R.; Mentink, S. *Nanotechnology* **2006**, *17*, 3779.

(10) Rotkina, L.; Oh, S.; Eckstein, J. N.; Rotkin, S. V. *Phys. Rev. B: Condens. Matter Mater. Phys.* **2005**, *72*, 233407.

(11) Puretz, J.; Swanson, L. W. *J. Vac. Sci. Technol., B* **1992**, *10*, 2695.

(12) Tao, T.; Ro, J.; Melngailis, J.; Xue, Z.; Kaesz, H. D. *J. Vac. Sci. Technol., B* **1990**, *8*, 1826.

(13) Donthu, S.; Pan, Z.; Myers, B.; Shekhawat, G.; Wu, N.; Dravid, V. *Nano Lett.* **2005**, *5*, 1710.

(14) Subramanian, K. R. V.; Saifullah, M. S. M.; Tapley, E.; Kang, D. J.; Welland, M. E; Butler, M. *Nanotechnology* **2004**, *15*, 158.

(15) Saifullah, M. S. M.; Subramanian, K. R. V.; Kang, D. J.; Anderson, D.; Huck, W. T. S.; Jones, G. A. C.; Welland, M. E. *Adv. Mater.* **2005**, *17*, 1757.

(16) Saifullah, M. S. M.; Subramanian, K. R. V.; Tapley, E.; Kang, D. J.; Welland, M. E.; Butler, M. *Nano Lett.* **2003**, *3*, 1587.

(17) Chuang, C. M.; Wu, M. C.; Huang, Y. C.; Cheng, K. C.; Lin, C. F.; Chen, Y. F.; Su, W. F. *Nanotechnology* **2006**, *17*, 4399.

(18) Wu, M. C.; Chuang, C. M.; Chen, Y. F.; Su, W. F. *J. Mater. Chem.* **2008**, *18*, 780.

(19) Werts, M. H. V.; Lambert, M.; Bourgoin, J. P.; Brust, M. *Nano Lett.* **2002**, *2*, 43.

10.1021/la803344f CCC: $40.75
Published on Web 12/18/2008

have been used as resists for metal nanopatterning. Werts et al.[19] demonstrated e-beam patterning on LB films of Au nanoparticles. Corbierre et al.[20,21] have used thiol terminated polystyrene to produce Au nanoparticle filled generated patterns. Patterning passivated nanocrystalline films of Au and Ag has been tried out to produce features down to 90 nm.[22] Reetz et al.[23] fabricated Pd and Pd/Pt nanostructures by exposing films containing corresponding cluster species to an e-dose of 0.2 $C \cdot cm^{-2}$ at 120 kV. Stark et al.[24] have reported e-beam induced Pd nanopatterns from palladium acetate. Recently, we have demonstrated the use of Pd hexadecanethiolate as a direct write resist for Pd metal patterning.[25] Upon thermolysis, the exposed resist yielded highly metallic patterns with the carbon impurity at record low ($<10\%$).

In the examples given above, all nanomaterial precursors behaved as negative-tone resists, implying that the exposed regions had less solubility in chosen solvents in contrast to unexposed regions. These are ready precursors for nanomaterial synthesis yet exhibiting cross-linking behavior similar to polymeric resists. Although there is enough literature on the behavior of polymeric resists, the direct write resists have not been studied in detail. As a model study, we considered it interesting to investigate the resist behavior of Pd hexadecanethiolate under different e-beam exposures. After having determined the thickness of the written patterns exposed to different e-beam conditions using an optical profiler, we have examined the chemical changes in the resist precursor employing core-level spectroscopy measurements at an ESCA microscopy synchrotron beamline. The results obtained have been corroborated with IR spectroscopy measurements. Our results show that the e-beam exposure induces facile nucleation of tiny Pd nanoparticles amidst organic ligands, containing defects.

Experimental Section

Preparation of Pd Hexadecanethiolate. Palladium hexadecanethiolate, $Pd(SC_{16}H_{35})_2$ was synthesized as follows: To 5.0 mmol of $Pd(OAc)_2$ (Sigma Aldrich) in toluene (7 mL), 5.0 mmol of hexadecanethiol (Sigma Aldrich) in toluene (3 mL) was added, and the resulting mixture was stirred vigorously.[26] Following the reaction, the solution became viscous and the yellow color deepened to orange yellow. The obtained thiolate as a dried powder was washed with methanol and acetonitrile to remove excess of thiol and finally dissolved in toluene to obtain a 0.1 mM solution. The solubility of Pd thiolate is clearly a novelty, as it enables further processing. This solution could be spin-coated as a smooth film of nanometric thickness and patterned.

Electron Beam Lithography and Characterization. For patterning using electron beam lithography (EBL), the Si substrates were cleaned by sonicating in acetone and double distilled water and dried under flowing argon. The resist film was made by spin-coating the Pd thiolate solution (0.1 mM) at 2000 rpm. The film thickness has been measured using a NT 1100 Wyko optical profilometer (Veeco Instruments). EBL was performed using an e-beam writer available with the scanning electron microscopy (SEM) equipment (FEI Nova NanoSEM 600 equipment, The Netherlands). An array of $10 \times 10\ \mu m^2$ square regions was exposed to an e-beam at 5 kV with different dosages (see scheme in Figure 1). The substrate was

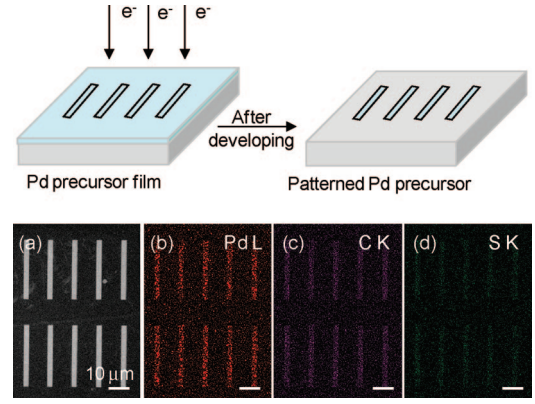

Figure 1. Scheme showing a Pd hexadecanethiolate film exposed to e-beam and developed in toluene for 10 s. (a) FESEM image and (b−d) EDS maps of Pd L, C K, and S K lines of the patterned regions. e-beam energy was 5 kV, and dosage was 54 $\mu C \cdot cm^{-2}$.

then developed in toluene for 10 s to dissolve away the unexposed resist. Thermolysis was carried out in air at 250 °C for 30 min. Energy dispersive spectroscopy (EDS) analysis was performed before and after the thermolysis, with an EDAX Genesis instrument (Mahwah) attached to the SEM column.

Scanning photoelectron microscopy (SPEM) with in situ heating of the specimen was performed at the ESCA microscopy beamline of Sincrotrone Trieste S.C.p.A. di Interesse Nazionale, Trieste, Italy. A Si substrate with e-beam patterned islands where the e-dosage has been varied from 2 to 280 $\mu C \cdot cm^{-2}$ was used without subjecting to thermolysis. Another substrate coated with a pristine Pd thiolate film was used for comparison. Photoemission spectra were measured with a spot size of about 150 nm, 500 eV photon energy, and 0.3 eV energy resolution which allows us to probe the core-level chemical shifts. Photoelectrons were detected by a hemispherical electron energy analyzer, under a fixed angle of 30° with respect to the surface plane, with an acceptance cone width of ±7°. The analyzer was equipped with a stripe detector for the simultaneous energy-dispersive detection in 48 channels. In the imaging mode, the sample is scanned by piezo-motors, yielding 48 images according to the number of parallel detection channels. Alternatively, in microspectroscopy mode, the analyzer energy set point is swept in order to take X-ray photoemission spectra from a well-defined, microscopic spot on the surface.[27,28] The spectra were also collected after subjecting the patterned substrate to thermolysis in the X-ray photoelectron spectroscopy (XPS) chamber for 10 min at 250 °C. For deconvolution of the XPS spectra, the background offset was of Shirley background type and the deconvolutions were performed using Origin 6.0 software using Gaussian functions with fwhm for the Pd and S species of 1.5 and 0.9 eV, respectively. The peak energy separation between spin orbit components was 5 eV for Pd and 1.2 eV for S,[29] with branching ratios of 3:2 and 2:1, respectively.

Fourier transform infrared measurements were performed using an IFS66v/s Bruker spectrometer with a resolution of $\sim 2\ cm^{-1}$ on a continuous film obtained by spin-coating the resist. For the measurements on the e-beam exposed film, an area of $3 \times 3\ mm^2$ was dosed (5 kV, 2 $\mu C \cdot cm^{-2}$). In order to perform transmission electron microscopy (TEM), a Cu holey grid was coated with the thiolate precursor, patterned with electron beam (5 kV, 2 $\mu C \cdot cm^{-2}$), developed in toluene, and thermolyzed at 250 °C. High-resolution TEM imaging was carried out with JEOL-3010 equipment operating at 300 kV.

(20) Corbierre, M. K.; Beerens, J.; Lennox, R. B. *Chem. Mater.* **2005**, *17*, 5774.
(21) Corbierre, M. K.; Beerens, J.; Beauvais, J.; Lennox, R. B. *Chem. Mater.* **2006**, *18*, 2628.
(22) Griffith, S.; Mondol, M.; Kong, D. S.; Jacobson, J. M. *J. Vac. Sci. Technol., B* **2002**, *20*, 2768.
(23) Reetz, M. T.; Winter, M.; Dumpich, G.; Lohau, J.; Friedrichowski, S. *J. Am. Chem. Soc.* **1997**, *119*, 4539.
(24) Stark, T. J.; Mayer, T. M.; Griffis, D. P.; Russell, P. E. *J. Vac. Sci. Technol., B* **1991**, *9*, 3475.
(25) Bhuvana, T.; Kulkarni, G. U. *ACS Nano* **2008**, *2*, 457.
(26) Thomas, P. J.; Lavanya, A.; Sabareesh, V.; Kulkarni, G. U. *Proc. Indian Acad. Sci., Chem. Sci.* **2001**, *113*, 611.
(27) Gunther, S.; Kaulich, B.; Gregoratti, L.; Kiskinova, M. *Prog. Surf. Sci.* **2002**, *70*, 187.
(28) Marsi, M.; Casalis, L.; Gregoratti, L.; Gunther, S.; Kolmakov, A.; Kovac, J.; Lonza, D.; Kiskinova, M. *J. Electron Spectrosc. Relat. Phenom.* **1997**, *84*, 73.
(29) Seah, M. P.; Briggs, D. *Practical Surface Analysis by Auger and X-ray Photoelectron Spectroscopy*, 2nd edition; Wiley & Sons: Chichester, U.K. 1992.

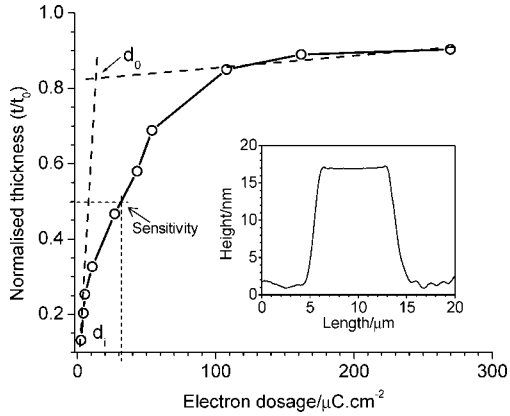

Figure 2. Film thickness, t, normalized to the initial film thickness t_0 (= 60 nm) against the e-dosage for the 5 kV e beam patterning. Inset shows the z-profile of a patterned region obtained from OP measurement (e-dosage, 11 $\mu C \cdot cm^{-2}$).

Results and Discussion

The Resist Action of Pd Hexadecanethiolate. While patterning of Pd hexadecanethiolate film has been carried out under varying e beam dosages (2−280 $\mu C \cdot cm^{-2}$), an example of the patterns is shown in Figure 1 obtained using a 5 kV e-beam with dosage of 54 $\mu C \cdot cm^{-2}$. From the field emission scanning electron microscopy (FESEM) image in Figure 1a, we see that the regions exposed to the e-beam remained on the substrate after developing in toluene, thus indicating the negative-tone resist behavior of the thiolate. The lines are 30 μm in length, 2 μm wide, and 60 nm thick. Corresponding to the FESEM image, the EDS images in Figure 1b−d show, as expected, the presence of Pd, C, and S, respectively, in the designated areas. The Pd/C/S elemental ratios (21:71:8) obtained for the patterned regions agrees with the initial composition (19:70:11) of the unexposed resist, $Pd(SC_{16}H_{35})_2$, implying that the e-dosage causes only minimal change in the overall composition. Such small changes can also occur due to carbon contamination during e-beam exposure.[30,31] Further, the variations in the Pd/C/S atomic ratios were within 5% for the different dosages. Importantly, the resist action of Pd hexadecanethiolate is evident.

At 5 kV with a beam current of 13 nA, squares of 10 × 10 μm^2 were patterned on a film of thickness ~60 nm while gradually varying the e-dosage from 2 to 280 $\mu C \cdot cm^{-2}$ (Figure 2). When examined under an optical profiler, the patterned regions were found to be quite smooth as the pristine region itself, an important feature of a high-resolution resist. Besides, the patterned regions failed to exhibit a high contrast, implying only a small variation in the thickness (<8%) following e-beam exposure. Following developing in toluene, however, square regions with clear contrast appeared which enabled thickness measurements across the boundaries. The inset of Figure 2 shows an example of the z-profile of a square pattern corresponding to a dosage of 11 $\mu C \cdot cm^{-2}$. The thickness of the developed region as measured using OP increased with the e-dosage, due to increasing resist action, from 7.8 nm at 2 $\mu C \cdot cm^{-2}$ to 54 nm at 280 $\mu C \cdot cm^{-2}$. In other words, at the minimum dosage value (2 $\mu C \cdot cm^{-2}$), only about 13% of the original thickness is retained following developing in toluene, and this value gradually increased to 85% beyond 120 $\mu C \cdot cm^{-2}$. From the plot in Figure 2, it is possible to deduce the sensitivity of the resist, which is defined as the dose at which half the thickness of the resist is preserved.[32] This value was found to be 32 $\mu C \cdot cm^{-2}$ for Pd hexadecanethiolate, which compared to other direct write resists is commendable. In the literature, typical values for Pd patterning are in the range of 1000 $\mu C \cdot cm^{-2}$.[23,24] The resolution achievable with a resist is defined in terms of its contrast parameter, γ: the higher the contrast, the higher the resolution.[33] For negative resist, $\gamma = 1/\log(d_0/d_i)$, where d_0 is the dose required to retain 100% of the resist material and d_i is the minimum dose at which resist action just begins.[34] For Pd hexadecanethiolate developed in toluene for 10 s (as in this experiment), the measured contrast value is 1.43 (see Figure 2).

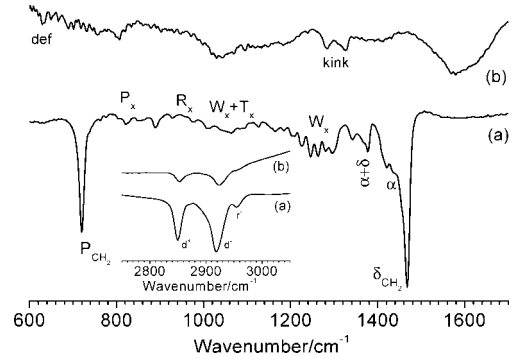

Figure 3. IR spectra of the (a) pristine and (b) e-beam exposed Pd hexadecanethiolate. The 2800−3000 cm^{-1} region is shown in detail in the inset.

In order to understand the resist action of Pd hexadecanethiolate, it is important to examine the changes in the conformations of alkyl chains on exposure to an e-beam. In Figure 3, we compare the IR spectra of the pristine Pd hexadecanethiolate film with the one exposed minimally to the e-beam (5 kV, 2 $\mu C \cdot cm^{-2}$). In the case of pristine thiolate (Figure 3, spectrum a), the wag-twist progression bands ($W_x + T_x$, 1175−1350 cm^{-1}) are well-defined, implying that the coupling between the methylene oscillators is unaffected because the chains are all-trans,[35−39] which is also evident from the C−H stretching modes (see inset of Figure 3). Interestingly, these bands are greatly diminished in intensity in the case of e-beam exposed film, which confirms the occurrence of gauche defects in the chains. The strong band at 1467 cm^{-1} due to the methylene scissoring mode (δ) seen in spectrum a is clearly absent in spectrum b, indicating that there is deformation in the alkyl chain on exposure of e-beam. Similar is the fate of the peak at 1419 cm^{-1} due to methylene deformation adjacent to the sulfur. The main band at 720 cm^{-1} is the head band of the rocking progression (spectrum a). This band is highly diminished in the case of e-beam exposed film (spectrum b). A series of peaks observed between 1000 and 1150 cm^{-1} are assigned to the skeletal C−C−C vibrational modes (R_x), while the progression bands in the region 700−980 cm^{-1} are assigned to the rocking modes (P_x) of the methylene chains that are more prominent in

(30) Vladár, A. E.; Postek, M. T.; Vane, R. *Proc. SPIE* **2001**, *835*, 4344.
(31) Vane, R.; Carlino, V. *Microsc. Microanal.* **2005**, *11*(Suppl 2), 900.
(32) Thompson, L. F.; Willson, C. G.; Bowden, M. J. *Introduction to Microlithography*; American Chemical Society: Washington, DC, 1994.
(33) Franssila, S. *Introduction to Microfabrication*; Wiley Publishers: New York, 2004.
(34) Brusatin, G.; Della Giustina, G.; Romanato, F.; Gulielmi, M. *Nanotechnology* **2008**, *19*, 175306.
(35) John, N. S.; Thomas, P. J.; Kulkarni, G. U. *J. Phys. Chem. B* **2003**, *107*, 11376.
(36) Maroncelli, M.; Qi, S. P.; Strauss, H. L.; Snyder, R. G. *J. Am. Chem. Soc.* **1982**, *104*, 6237.
(37) Seshadri, K.; Froyd, K.; Parikh, A. N.; Allara, D. L.; Lercel, M. J.; Craighead, H. G. *J. Phys. Chem.* **1996**, *100*, 15900.
(38) Snyder, R. G.; Maroncelli, M.; Qi, S. P.; Strauss, H. L. *Science* **1981**, *214*, 188.
(39) Suresh, R.; Venkataraman, N.; Vasudevan, S.; Ramanathan, K. V. *J. Phys. Chem. C* **2007**, *111*, 495.

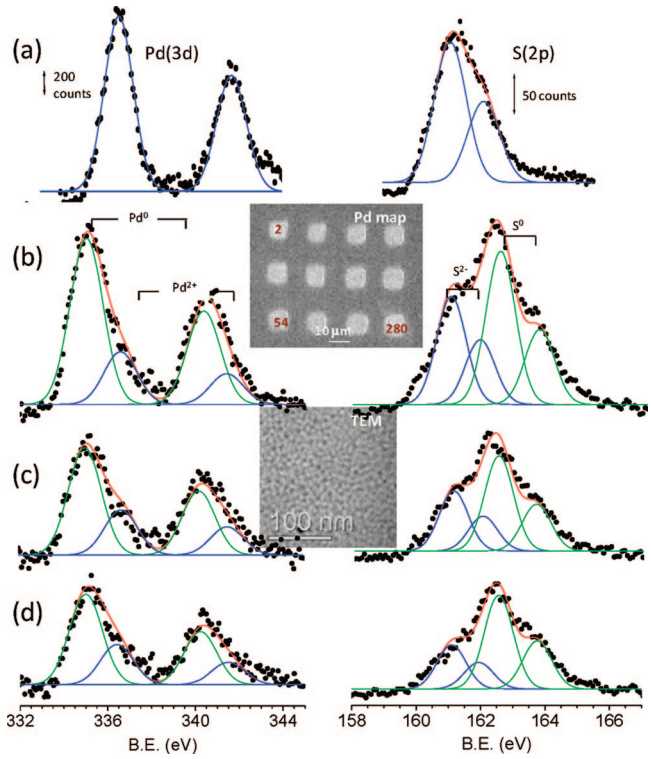

Figure 4. (a) Pd(3d) and S(2p) core-level spectra of the pristine film. Spectra corresponding to the patterned islands subjected to 2, 54, and 280 $\mu C \cdot cm^{-2}$ dosages are shown in (b), (c), and (d), respectively. The e-beam energy was 5 kV. Inset in (b) shows core-level mapping of an array of Pd islands where the chosen islands have been marked. TEM image showing the formation of fine Pd nanoparticles on exposure to e-beam (54 $\mu C \cdot cm^{-2}$) is in the inset in (c).

spectrum b. Importantly, spectrum b exhibits weak bands at 1321 and 1365 cm^{-1} due to $W_{g\text{-}t\text{-}g}'$, indicating the presence of kinks in the chain, due to exposure to the e-beam. There is a broad peak observed around 1650 cm^{-1} in spectrum b, due to the loss of hydrogen atoms and radical formation leading to double bonds. This is also an indication of cross-linking of the chains, important in resist action.[37] The characteristic C−H stretches of the methylene and end-methyl groups of the alkane chain appear in the 2800−3000 cm^{-1} region (see inset of Figure 3). In the case of pristine thiolate, the symmetric (d^+) and antisymmetric (d^-) methylene C−H stretching modes are broad with the mean positions at 2848 and 2918 cm^{-1}, respectively. A shift of 4 cm^{-1} in the vibrational frequency implies a disordered environment, such as gauche defects in the thiolate film exposed to e-beam (spectrum b in the inset). The r^- (methyl antisymmetric stretch) modes appear around 2960 cm^{-1}, which also diminishes on exposure to the e-beam and appears as a high frequency shoulder, indicating that most methyl groups have been damaged and/or removed.[39] Clearly, the e-beam exposure induced deformations and cross-linking of the alkyl chains of Pd thiolate make it less soluble during developing and thus an electron sensitive resist.

Nanospectroscopy Measurements. In order to study the chemical changes on Pd thiolate on exposure to e-beam, XPS analysis using a nanospectroscopy beamline was carried out on e-beam patterned islands where the e-dosage has been varied from 2 to 280 $\mu C \cdot cm^{-2}$, as well as on a pristine Pd thiolate film for comparison (Figure 4). Pd(3d) and S(2p) core-level spectra recorded on the pristine film show the presence of Pd^{2+} ($3d_{5/2}$ at 336.6 eV and $3d_{3/2}$ at 341.6 eV) and S^{2-} ($2p_{3/2}$ at 161 eV and $2p_{1/2}$ at 162.2 eV) species as expected. Among the 12 islands patterned, three were chosen to study the trend, namely, 2, 54, and 280 $\mu C \cdot cm^{-2}$, being the lowest, intermediate, and highest

Scheme 1. (I) Pd Hexadecanethiolate Containing Pd^{2+} (Blue) Species; (II) the Film Is Exposed to Different e-Beam Dosages in Different Regions; (III) the e-Beam Is Reducing Pd^{2+} to Pd^0 (Red), It Is Expected That the Reduction Is More at High e-Dosages; (IV) Pd^{2+} and Pd^0 Species after Developing the Exposed Resist; Pd^0 Species Gets Washed Away More Easily from the Region Exposed to High e-Dosages

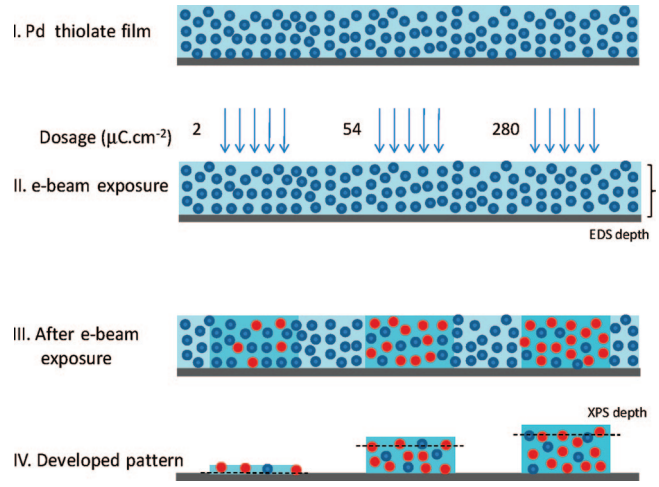

dosages employed. These have been marked in the core-level map of the patterned region as shown in the inset of Figure 4. Surprisingly, in all three cases, the Pd(3d) main peak is positioned at ~335 eV, indicating the predominant presence of the metallic species Pd^0. This is the first important finding from the nano-XPS measurements. A TEM image on the 54 $\mu C \cdot cm^{-2}$ patterned region (see lower inset of Figure 4) shows the formation of fine particles below 5 nm diameter. Indeed, the e-beam exposure not only brings about chain defects and deformation (as evidenced from IR measurements in Figure 3) but also causes significant reduction of Pd^{2+} to Pd^0. Following deconvolution into Pd^0 (335 and 340 eV) and Pd^{2+}, we observe that the ratio, Pd^0/Pd^{2+}, varies in a narrow range, 3.10−2.25, with e-dosage. More precisely, the ratio decreases with an increase in e-dosage, 3.10, 2.28, and 2.25 at 2, 54, and 280 $\mu C \cdot cm^{-2}$, respectively. Furthermore, the intensity of the Pd^0 component decreases with increasing e-dosage. This suggests that, during developing of the resist, the metallic species produced with higher e-dosage gets washed away relatively easily. Second, we notice that the overall spectral intensity decreases with increasing e-dosage. The loss of total Pd species is relatively more compared to S species. Such sensitive variations could be detected with nano-XPS, which was not the case with the EDS measurements. On the contrary, the C(1s) spectra showed no variation in the spectral intensity (spectra not shown). From the above observations, it may be deduced that, following developing, the carbon content in the surface layers remains similar irrespective of the e-dosage, while Pd does not; e-beam induces reduction and formation of the metallic species, but some of it is lost during developing of the resist, particularly from regions exposed to higher dosages. The unreduced Pd^{2+} is lost but to a lesser extent. The S(2p) spectra show a similar trend as Pd(3d). Here, S^0 (162.5 and 163.7 eV) is predominant but decreases with increasing e-dose relative to S^{2-} (161 and 162.2 eV), with the ratio being 0.70, 0.67, and 0.47 at 2, 54, and 280 $\mu C \cdot cm^{-2}$, respectively. Scheme 1 shows the effect of e-beam on the resist for different dosages. As shown, initially the resist contains only Pd^{2+} species (blue balls) (step I). On exposure to the e-beam (step II), reduction of Pd^{2+} to Pd^0 (red balls) takes place. On increasing the e-dosage, the extent of reduction of Pd^{2+} species to Pd^0 is higher (step III), but while developing the

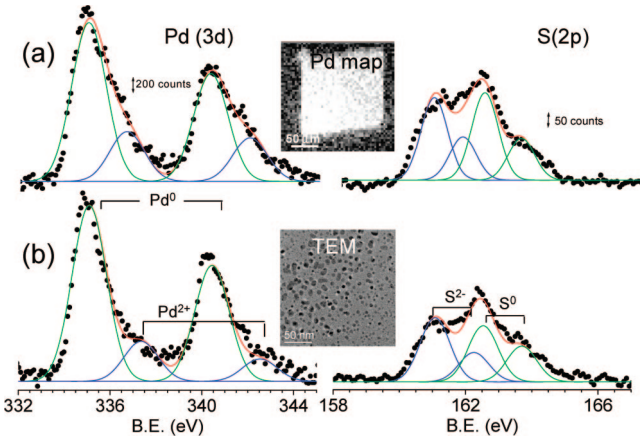

Figure 5. Pd(3d) and S(2p) core-level spectra of a big island (250 × 220 μm^2) patterned with a 5 kV beam at 2 $\mu C \cdot cm^{-2}$ and subjected to in situ thermolysis at (a) 160 °C and (b) 250 °C. Top inset: Pd core-level mapping of the island. The image looks slightly distorted due to a mechanical drift of the substrate while in situ heating. TEM image of patterned Pd after thermolysis at 250 °C is shown in the bottom inset.

patterned resist (step IV) some of the Pd species get washed away, particularly Pd^0 from regions exposed to high dosages.

Here, we observe countering effects of e-dosage on our direct write resist. While a higher dosage does induce more resist action (in terms of defect formation and cross-linking resulting in higher thickness of the resist retained), it also makes the resist more vulnerable to developing, as the reduced Pd species are more likely to get washed away as compared to the charged species. Unlike in the case of a conventional polymer resist, a higher contrast alone is not sufficient for a direct write resist. A predominant presence of the active precursor is important, and in this sense the optimal parameters for a direct write precursor would be different from those of conventional resists. Under the given conditions, a dose of over 100 $\mu C \cdot cm^{-2}$ can retain up to 85% of the resist thickness. Based on the spectral intensities in XPS, this translates to a total Pd content that is nearly 1.5 times that retained at sensitivity value (32 $\mu C \cdot cm^{-2}$).

While the resist action is conventionally associated with cross-linking and reduced solubility during developing, the e-beam exposure bringing about reduction of Pd^{2+} to metallic species is a novel feature of this direct write resist. The reduction brought about by the e-beam can be further enhanced by thermolysis. It may recalled that many noble and seminoble metal alkanethiolates upon thermolysis give up the organic component and reduce to metallic species.[40] In Figure 5, we show Pd(3d) and S(2p) core-level spectra from a 250 × 220 μm^2 patterned area (using 5 kV and e-dosage 2 $\mu C \cdot cm^{-2}$) while subjected to increasing temperatures in the XPS chamber. The image in the top inset is a Pd core-level map. Prior to thermolysis, the room temperature spectra of the e-exposed resist gave Pd^0/Pd^{2+} and S^0/S^{2-} values of 3.14 and 0.47, respectively, similar to the spectra shown in Figure 4b. As noted, there is already a significant amount of metal present in the pattern brought about by e-beam exposure. Upon heating the substrate to 160 °C for 5 min (see spectra in Figure 5a), the relative content of Pd^0 increased (3.6) with the concomitant S^0 state (1.14). The content of metallic species further increased (Pd^0/Pd^{2+}, 4.5) after holding the substrate temperature at 250 °C for 10 min (Figure 5b).

(40) Nakamoto, M.; Yamamoto, M.; Fukusumi, M. *Chem. Commun.* **2002**, 1622.

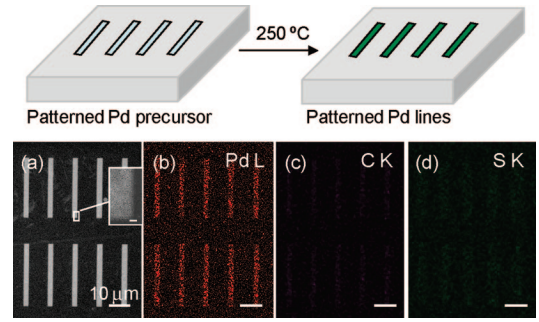

Figure 6. Scheme showing ex situ thermolysis of the patterned resist. (a) FESEM and (b−d) EDS maps of Pd L, C K, and S K lines on the e-beam patterned regions shown in Figure 1, after thermolysis in air at 250 °C for 30 min. Inset in (a) shows a magnified image of the patterned line. Scale is 200 nm.

Accordingly, the TEM image (inset in Figure 5b) showed the presence of Pd nanocrystals in the size range of 5−15 nm. This TEM image may be contrasted with that shown in Figure 4. Following thermolysis, the growth of Pd nuclei formed during EBL is evident. The Pd^{2+} and S^{2-} species seen after thermolysis correspond mostly to the surface species.

The reduction and growth of the Pd metallic species can be carried out by thermolysis in air[25] as well (see the Supporting Information). In Figure 6, we show FESEM and EDS images after ex situ thermolysis at 250 °C. The lateral morphology of the pattern is intact, but the thickness was reduced from 60 to ∼35 nm. Pd L EDS mapping (Figure 6b) shows the presence of Pd in the designated regions similar to that in Figure 1b. However, the C K and S K signals became significantly weaker following thermolysis (compare Figure 6c and d with Figure 1c and d, respectively), with a Pd/C/S ratio of 89.7:9.8:0.5 suggesting loss of thiol in the patterned regions. Some of the carbon signal may arise due to contamination during SEM/EDS measurements, and the actual value may be much less. The inset in Figure 6a shows the details of the patterned region; the boundaries are seen as sharp and well-defined.

Conclusions

We have studied the electron resist behavior of Pd hexadecanethiolate in direct write electron beam lithography. As a metal precursor readily soluble in organic media, it could be spin-coated as a smooth thin film on Si substrate. With the e-beam energy set at 5 kV, 10 × 10 μm^2 regions of the film were given varying doses, 2−280 $\mu C \cdot cm^{-2}$. Following developing in toluene (10 s), the exposed regions remained on the substrate, qualifying the precursor as a negative-tone resist. The thickness of the patterned squares varied with e-dosage. From the plot of the thickness versus dosage, a sensitivity value of 32 $\mu C \cdot cm^{-2}$ and a contrast parameter of 1.43 were obtained for the resist. Core-level spectra of the patterned regions collected on a synchrotron beamline showed the predominant presence of Pd^0 along with Pd^{2+} from the precursor, with the ratio of Pd^0/Pd^{2+} being relatively high at low dosages, 3.1 at 2 $\mu C \cdot cm^{-2}$ as against 2.25 at 280 $\mu C \cdot cm^{-2}$. Further, the overall intensity of the Pd(3d) decreased with increasing dosage. Similar observations have been made with respect to S states, S^0 and S^{2-}. However, the C(1s) signal intensity showed negligible change with the e-dosage. The above observations imply that, with increasing dosage, there is more reduction in the resist, from Pd^{2+} to Pd^0, but some of it gets washed away during developing. However, since the thickness retained is more at higher dosages, higher

dosages are to be preferred, with the optimal value being $\sim 100\ \mu C \cdot cm^{-2}$. Thermolysis of the patterned regions at 250 °C yielded metallic Pd patterns as revealed by TEM and core-level photoelectron spectroscopy measurements.

Acknowledgment. The authors are grateful to Professor C. N. R. Rao for his encouragement. Thanks are also due to Veeco India Nanotechnology Laboratory, JNCASR, for providing the optical profilometer facility. Support from the Department of Science and Technology, Government of India, is gratefully acknowledged. S.H. and GUK acknowledge support from the Indo-Italian POC in S&T 2005−2007. T. B. thanks Utilization of International Synchrotron Radiation and Neutron Scattering facilities (A project supported by the Department of science and Technology Government of India) for the travel support.

Supporting Information Available: FESEM image of a thermolysed Pd hexadecanethiolate film without e-beam patterning. This material is available free of charge via the Internet at http://pubs.acs.org.

LA803344F